Argonne NATIONAL LABORATORY

ANL-20/83

Development and Optimization of a Purification Process to Recover ^{99}Mo from Low-enriched Uranium

Chemical & Fuel Cycle Technologies Division

ANL-20/83

Development and Optimization of a Purification Process to Recover ^{99}Mo from Low-enriched Uranium

by
M. Alex Brown, Anna Servis, and Peter Tkac
Chemical & Fuel Cycle Technologies, Argonne National Laboratory

December 2020

CONTENTS

FIGURES

TABLES

1 INTRODUCTION

Supported by the DOE-NNSA Office of Material Management & Minimization (M3), a number of domestic entities are pursuing non-highly enriched uranium (non-HEU) production of ^{99}Mo. As the production technologies of 99Mo pivot toward low-enriched uranium (LEU) or molybdenum targets, new reaction channels and accelerators are being evaluated. Superconducting electron linear accelerators (LINACs) with high-Z converter targets can generate bremsstrahlung photons and neutron fluxes that are capable of inducing photonuclear reactions and LEU fission.[1] A particular advantage of a LINAC is that it does not rely on HEU-fueled reactor cores (which are currently slated for LEU conversion) and can operate on an almost continuous basis.

Regarding the chemical purification of ^{99}Mo from irradiated uranium targets under acidic digestion, there exists a procedure known as Cintichem or modifications thereof with respect to LEU (LEU Modified Cintichem process, LMC).[2, 3] The process relies on a number of selective precipitation steps and column chromatography to purify Mo. It is important to note that LMC prescribes the addition of stable Mo to carry ^{99}Mo on alpha benzoin oxime, which reduces the specific activity of ^{99}Mo. This is especially important for processing ^{99}Mo batches with lower activities (~33 Ci of ^{99}Mo per batch).

A new chemical purification procedure is being sought that can treat irradiated uranium targets for the recovery of high-specific activity ^{99}Mo. To be viable, the procedure must address the following requirements: (1) rapid execution with minimal precipitation and filtration steps; (2) no addition of stable carrier elements, as to not subvert the high-specific activity of valuable fission products; and (3) a method that is mindful of the need to recover LEU target material. To facilitate these requirements, we derived a separation scheme that relies primarily on solvent extraction. This approach results in excellent front-end removal and back-end recovery of uranium (UREX, uranium extraction) in dilute acids where “dilute” indicates an acid concentration of 0.5–5 M HNO_3. The concentration of HNO_3 following UREX is slightly lower on account of HNO_3 extraction by tri-n-butyl phosphate (TBP) and is estimated to be anywhere between 1 and 2 M. Second, the solvent extraction of Mo by an organophosphoric or phosphonic acid from nitric acids (MoLLE, Molybdenum Liquid–Liquid Extraction,) is capable of decontaminating Mo from a mixture of fission products born out of a UREX raffinate.[4, 5] Similar process chemistry was recently utilized to selectively remove Mo during the recovery of minor actinides in spent nuclear fuel.[6] The advantages of this combined approach (UREX + MoLLE) include maintaining solubility during purification steps and the potential to execute these process stages using continuous flow equipment such as high-throughput countercurrent centrifugal contactors. For a final purification and concentration step, an anion-exchange column yields low-volume, high-specific-activity $^{99}MoO_4^{2-}$ in a simple alkaline matrix.

This work summarizes the development of a chemical process to quickly recover high-specific activity ^{99}Mo from irradiated uranium. Following the dissolution or reconstitution of the uranium in 3 M HNO_3, the irradiated targets were treated under the process flowsheet shown schematically in Figure 1. Slight iterations were made to the concentrations, volumes, or selected reagents to optimize each stage. The results and discussion will focus on detailed aspects

surrounding UREX, MoLLE, and the concentration column in order to achieve high-purity, high-specific-activity ^{99}Mo.

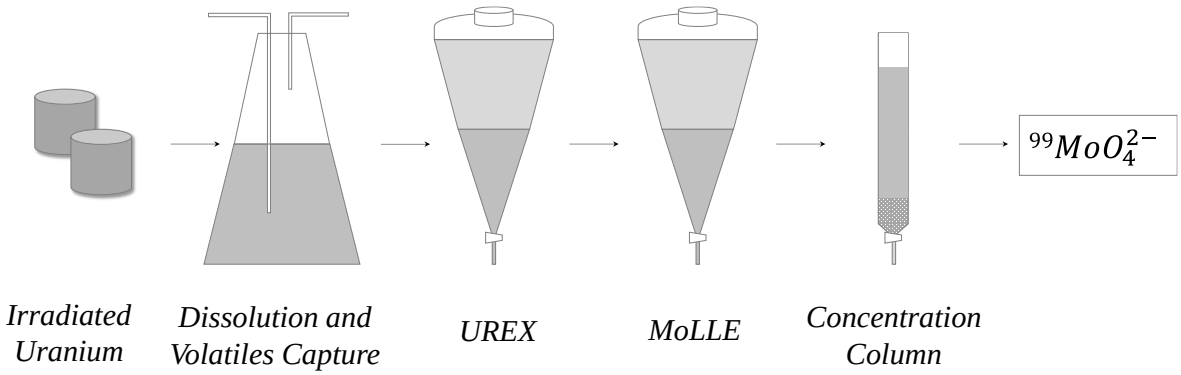

FIGURE 1 Niowave Process Overview.

2 METHODS

2.1 REAGENTS

Organic solutions were prepared with either >99% TBP (Sigma Aldrich) or 97% di-2-ethylhexyl phosphoric acid (HDEHP; Sigma-Aldrich) and 99+% *n*-dodecane (Alfa Aesar). Deionized (DI) water with a resistivity of 18.2 MΩ·cm was used in the preparation of all aqueous solutions. Other reagents used include trace element grade concentrated nitric acid (Fisher Scientific), trace element grade concentrated hydrochloric acid (Fisher Scientific), oxalic acid dihydrate (certified ACS, Sigma Aldrich), sodium chloride (>99%, Sigma Aldrich), 50% NaOH in water (Sigma Aldrich), acetohydroxamic acid (AHA; 98%, Acros Organics), sodium nitrate (99+%, Alfa Aesar), and ammonium molybdate(VI) tetrahydrate (ACS reagent, Fisher Scientific).

Fission product radiotracer spikes were prepared by diluting a solution consisting initially of 140 g U/L as uranyl sulfate in pH 1 H_2SO_4 that had been irradiated at the Low Energy Accelerator Facility (LEAF)[2] in a 1:4 volume ratio with 0.5 M HNO_3. A radiotracer solution containing ^{99}Mo was obtained by milking molybdenum from a 1 Ci ^{99m}Tc generator with 1 M NH_4OH.

Stable Sb(V) and Sn(II) spike solutions were prepared by dissolving their chloride compounds in nitric acid. Both elements tend to form insoluble species at moderate nitric acid concentrations, so fresh solutions were prepared immediately before performing experiments. The antimony solution was prepared by dissolving approximately 0.4 g $SbCl_3$ (Chem Service, Inc.) in 3 mL concentrated HNO_3 and diluting the resulting solution tenfold with concentrated HNO_3. This solution was then diluted 20× with DI water. The starting Sb(III) is known to oxidize rapidly to Sb(V) in nitric acid solutions. The tin solution was prepared by dissolving $SnCl_2$ (98%, Sigma Aldrich) in HNO_3 and DI water to reach a final concentration of 0.1 M Sn in 1 M HNO_3.

A natural molybdenum metal disc was irradiated at the LEAF to produce ^{99}Mo, ^{95}Nb, ^{95}Zr, and ^{88}Y tracers.[7] The disc was processed using H_2O_2 and NaOH and used for fission product separation studies.

2.2 AMUSE AND U/MO DECONTAMINATION

Niowave intends to first process uranium targets using a nitric acid-based process with TBP in a hydrocarbon diluent. On the front end, this step removes the bulk uranium (and selected actinides and fission products) from 3 M HNO_3. On the back end, uranium can be recovered in pH 2 nitric acid as a precursor for target recovery and re-fabrication. This process can be scaled up with countercurrent centrifugal contactors to increase throughput; therefore, it is important to develop and optimize a solvent extraction flowsheet that provides high degrees of decontamination and recovery.

Argonne manages software titled AMUSE (Argonne Model for Universal Solvent Extraction) that uses fundamental thermodynamic constants and experimental data to simulate the extraction of ions from nitric acid. This code can be used to develop flowsheets with known actinide and fission product inputs. The flowsheets can be optimized with respect to (1) number of stages, (2) aqueous and organic phase flowrates, and (3) reagent concentrations to achieve desired purity levels and temperature.

2.3 BATCH LIQUID-LIQUID DISTRIBUTION STUDIES

Distribution studies were performed for TBP and HDEHP liquid–liquid extraction systems to determine the equilibrium extraction behavior of uranium fission products under relevant process conditions. These include experimental conditions investigating extraction from an aqueous phase at various HNO_3 concentrations and stripping from an HDEHP organic phase at various AHA concentrations. An organic phase consisting of either 30 v/v% TBP or 0.4 M HDEHP in dodecane was used for all experiments. Organic phases were preequilibrated with an equal volume of a metal-free aqueous phase corresponding to each experimental condition to ensure a constant phase volume during each contact.

A 1:1 organic to aqueous phase ratio was used in all experiments. First, 600 µL of the preequilibrated organic phase and 600 µL of the metal-free aqueous phase were combined in a 2-mL microcentrifuge tube. A small, metal-containing spike less than 50 µL in volume was then added to each vial as needed to reach the desired sample count rate or metal concentration and the vials were shaken by hand for 5 minutes. The phases were allowed to separate by gravity for at least 30 minutes. Samples of each phase were then collected for analysis by either gamma spectroscopy or inductively coupled plasma mass spectrometry (ICP-MS), depending on whether the spike contained a radiotracer or a stable compound. The counting error in samples analyzed by gamma spectroscopy was less than 5%. The estimated error in metal concentrations determined by ICP-MS was less than 10%. A summary of the experimental conditions used is provided in TABLE 1.

TABLE 1 Process-relevant Experimental Conditions.[a]

Elements	Form	Organic Phase	Aqueous Phase
Sn, Sb	Stable Compounds	30 v/v% TBP in dodecane	0.5–4 M HNO_3
Nb, Zr, Mo, I, Ru, La, Ce	Radiotracers	0.4 M HDEHP in dodecane	0.5–4 M HNO_3
Sn, Sb	Stable Compounds	0.4 M HDEHP in dodecane	0.5–4 M HNO_3
Nb, Zr, Mo, Ru, Ce	Radiotracers	0.4 M HDEHP in dodecane	0.1–1.5 M AHA

[a] Distribution ratios were measured under these conditions.

When radiotracers were used, the distribution ratio (*D*) for each element was calculated using Equation (1), where $C_{n,\mathrm{org}}$ is the final organic phase decay corrected count rate and $C_{n,\mathrm{aq}}$ is the final aqueous phase decay corrected count rate for each radionuclide, n, in 300 µL samples of each phase. The gamma peaks observed in the newly irradiated fission product solution are reported in Table 2.

$$D = \frac{C_{n,\mathrm{org}}}{C_{n,\mathrm{aq}}} \tag{1}$$

When stable compounds were used, the distribution ratio (*D*) for each element was calculated using Equation (2), where $[M]_i$ is the initial aqueous phase concentration of each element *M* and $[M]_{\mathrm{aq}}$ is the final aqueous phase concentration. This equation is only valid when a 1:1 organic to aqueous phase ratio is used.

It is important to note that using only final aqueous phase metal concentrations or count rates to calculate distribution ratios results in substantial uncertainties (more than 100% for a 1% uncertainty in concentration) when the distribution ratios are less than 10^{-1}.

$$D = \frac{[M]_i - [M]_{\mathrm{aq}}}{[M]_{\mathrm{aq}}} \tag{2}$$

TABLE 2 Peak Energies for Radionuclides.[a]

Radionuclide	Peak Energy (keV)
^{132}Te	49.7
^{141}Ce	145.4
^{239}Np	277.6
^{131}I	364.5
^{235}U	185.7
^{103}Ru	497.08
^{140}Ba	537.26
^{99}Mo	739.5
^{95}Zr	756.7
^{95}Nb	765.8
^{140}La	1596.21

[a] Gamma spectroscopy was used to determine the decay-corrected count rates at these peak energies.

2.4 PHASE DISENGAGEMENT STUDIES

Characterizing phase disengagement and the nature of the emulsion is important when developing new liquid–liquid processes.[8] Extraction systems forming aqueous-organic dispersions with lifetimes longer than the residence time in continuous solvent extraction equipment are impractical for use in applied separations. Phase disengagement studies were performed to determine the impact of AHA concentration, AHA solution age, HNO_3 concentration, and HDEHP preequilibration on the phase disengagement time. For each experimental condition, a glass screw cap test tube with outer dimensions of 100 × 13 mm was first filled with 3 mL of an aqueous phase. The location of the aqueous interface was then noted by drawing a horizonal line halfway between the elevated outer edge of the meniscus and its central minimum with a permanent marker. An equal volume of organic phase was carefully pipetted into the test tube such that the interface between the two phases was not disturbed. The total height of the two phases in the test tube was measured as 6.7 cm. The test tube was then shaken by hand for a count of 5 (approximately 10 shakes) and the separation of the phases was captured by digital camera. Following complete separation and clarification of the phases, the shaking step was repeated.

Where possible, both organic continuous and aqueous continuous dispersions were produced for each experimental condition. Organic continuous dispersions were identified by the presence of aqueous droplets in the organic phase following the bulk separation of the two phases. Similarly, aqueous continuous dispersions were identified by the presence of organic droplets in the aqueous phase. It was observed for the conditions explored here that if a single, full test tube was shaken and allowed to separate twice in series, the first 5-second shake would usually result in an organic continuous dispersion, while the second shake would result in an aqueous continuous dispersion.

To determine phase disengagement time, digital videos of each sample were reviewed. The phase disengagement times reported here correspond to the time at which the bulk of each phase was fully separated and the interface between the phases was at its original position to within 2–3 mm. Bulk phase separation in aqueous continuous dispersions was often observed to reach completion with the aqueous phase remaining cloudy, which would then become completely transparent after several more hours or days.

The dimensionless dispersion number, a quantity used in the design of centrifugal contactors, was calculated for each sample according to Equation (3), where N_{Di} is the dimensionless dispersion number, t_B is the time required for phase disengagement, a is the acceleration experienced by the phases (equal to gravity, 9.81 m/s^2, in this experiment), and Δz is the initial thickness of the dispersion (6.7 cm). A dispersion number greater than 1.6×10^{-3} suggests excellent compatibility with continuous solvent extraction equipment, while a number greater than 8×10^{-4} exhibits good compatibility. Dispersion numbers less than 4×10^{-4} and 2×10^{-4} are fair and poor, respectively.[8]

$$N_{Di} = \frac{1}{t_B}\sqrt{\frac{\Delta z}{a}} \tag{3}$$

2.5 ^{99}MO SEPARATION DEMONSTRATION FROM LEU TARGETS

The overall process as a whole consists of three main parts: the recovery of uranium for reuse by TBP extraction (the UREX process), the recovery of ^{99}Mo by HDEHP extraction and AHA stripping (the MoLLE process), and the final decontamination of the ^{99}Mo product by anion exchange. The primary goal of the first step, which uses established UREX process chemistry, is to completely recover the LEU making up the irradiated target for fabrication into new targets. The second step is used for gross decontamination of the ^{99}Mo product from the majority of the remaining fission products. The final anion exchange column is a final polishing step with the primary goal of removing the remaining fission products, mostly niobium, and a secondary goal of concentrating the ^{99}Mo product.

The starting material for these bench scale investigations was the same 140 g U/L uranyl sulfate solution used in the fission product spike solution described previously, added to 1.3 M uranyl nitrate in 3 M HNO_3 in an amount making up less than 10% of the total starting solution

volume. It was assumed that the minor sulfate component in these solutions, which is less than 2% of the final anion inventory, would have a minimal impact on the process chemistry.

First, the initial uranyl nitrate solution was contacted three times with 30 v/v% TBP in dodecane to remove the uranium from the aqueous phase. The resulting aqueous raffinate was then contacted two times with 0.4 M HDEHP in dodecane organic phase to extract the molybdenum. The molybdenum was stripped to aqueous solution using a 0.5 M AHA solution. The pH of the strip solution was then adjusted to 12 with concentrated NH_4OH and loaded on a 1-cm inner diameter gravity-fed anion exchange column prepared with 1 g of the chloride form of AG 1-X8 (100–200 mesh) preequilibrated with 1 M NH_4OH. The remaining fission product impurities were eluted with NaOH, HCl/oxalate, and HCl washes. The purified ^{99}Mo was then stripped from the column with a 1 M NaOH/1 M NaCl solution. The volumes and concentrations of reagents used in the two runs are summarized in TABLE 4 and TABLE 5. For the first run, only the UREX raffinate, AHA strip, and each column wash were analyzed by gamma spectroscopy with a well-type high-purity germanium detector. For the second run, subsamples of the solutions at each step were collected and analyzed by gamma spectroscopy with a coaxial high-purity germanium (HPGe) detector. The radionuclides and corresponding peak energies analyzed are provided in Table 2

TABLE 3 Experimental Conditions Used in the First Complete Process Experiment.[a]

Description	Initial Aqueous Phase or Wash Used	Aqueous Vol. in mL (No. of Stages or Washes)	Initial Organic Phase Used	Organic Vol. in mL (No. of Stages or Washes)
UREX Extraction	1.3 M $UO_2(NO_3)_2$ and fission products in 3 M HNO_3	3 (3)	30 v/v% TBP (not preequilibrated)	5 (3)
MoLLE Extraction	Fission products and ≈1 M HNO_3	3 (2)	0.4 M HDEHP (not preequilibrated)	2 (2)
MoLLE Strip	0.3 M AHA	2 (2)	Fission products and 0.4 M HDEHP	2 (2)
Column Loading	Fission products, 0.3 M AHA, pH 12	10 (1)		
Column NaOH Wash	0.1 M NaOH	10 (1)		
Column NaOH Wash	1 M NaOH	10 (1)		
Column HCl/Oxalate Wash	5 M HCl/0.2M oxalic acid	10 (4)		
Column HCl Wash	4 M HCl	10 (2)		
Column NaOH/NaCl Strip	1 M NaOH/1 M NaCl	10 (2)		

[a] Samples were collected of the UREX raffinate, AHA strip, and each column wash for gamma counting on a well-type HPGe detector.

TABLE 4 Experimental Conditions Used in the Second Complete Process Experiment.[a]

Description	Initial Aqueous Phase or Wash Used	Aqueous Vol. in mL (No. of Stages or Washes)	Initial Organic Phase Used	Organic Vol. in mL (No. of Stages or Washes)
UREX Extraction	1.3 M $UO_2(NO_3)_2$ and fission products in 3 M HNO_3	4.5 (3)	30 v/v% TBP (preequilibrated)	6.75 (3)
MoLLE Extraction	Fission products and ≈1 M HNO_3	3.5 (2)	0.4 M HDEHP (preequilibrated)	1.75 (2)
MoLLE Strip	0.5 M AHA	2.5 (2)	Fission products and 0.4 M HDEHP	2.5 (2)
Column Loading	Fission products and 0.5 M AHA, pH 12	5 (1)		
Column NaOH Wash	1 M NaOH	10 (1)		
Column HCl/Oxalate Wash	5 M HCl/0.2M oxalic acid	10 (4)		
Column HCl Wash	4 M HCl	10 (2)		
Column NaOH/NaCl Strip	1 M NaOH/1 M NaCl	10 (2)		

[a] Samples were collected at each step for gamma counting on a coaxial HPGe detector.

2.6 THIOCYANATE EXTRACTION FOR ASSESSING ^{99}MO RADIONUCLIDIC PURITY

The ^{99}Mo product derived from the concentration column was tested for radionuclidic purity. Molybdenum can be selectively extracted as the Mo(V) thiocyanate complex to allow for the detection of unextractable very low activity fission product impurities by reducing the background gamma activity generated by the major component, ^{99}Mo. First, 6 mL ethyl acetate was preequilibrated with an aqueous phase consisting of 0.1 mL 0.1 M NaOH, 1 mL 1.8 M H_2SO_4, 0.1 mL 6.6 M NH_4SCN, 0.25 mL 0.44 M $SnCl_2$ in 1.2 M HCl, and 0.05 mL 0.075 M $Fe_2(SO_4)_3$ in 0.18 M H_2SO_4. To prepare for extraction, 0.2 mL of the ^{99}Mo product was combined with 0.02 mL of a 0.2 mM Rh/0.1 mM Ru/3 mM Mo carrier solution, 2 mL 1.8 M H_2SO_4, 0.2 mL 6.6 M NH_4SCN, 0.5 mL 0.44 M $SnCl_2$ in 1.2 M HCl, and 0.1 mL 0.075 M $Fe_2(SO_4)_3$ in 0.18 M H_2SO_4. This solution was contacted with 2.5 mL, then 1 mL, of the preequilibrated ethyl acetate. The organic phase was removed and discarded following each contact. A 2-mL sample of the aqueous phase was collected for overnight gamma counting in a well-type HPGe detector.

Because no impurity peaks were evident in the collected gamma spectrum, the minimum detectable activity (MDA) of the trace impurity ^{103}Ru was calculated according to Equation (4), where n is the number of channels in the gamma peak (when observed), m is the number of channels on either side of the peak whose counts are included in the background, B is the number of counts in the $n + 2m$ channels under the peak, not including the peak counts, ε is the detector efficiency, P_γ is the gamma-ray emission probability, and t_L is the detector live time during the count.[9]

$$\mathrm{MDA} = \frac{2.71 + 3.29\sqrt{B(1 + n/2m)}}{\varepsilon \times P_\gamma \times t_L} \quad (4)$$

2.7 BATCH SOLID-LIQUID DISTRIBUTION STUDIES

Solid–liquid distribution studies were performed to aid in the optimization of column preparation and elution conditions. A molybdenum adsorption isotherm at 25°C for the hydroxide form of AG 1-X8 resin (200–400 mesh) was constructed by varying the initial molybdenum concentration in a 0.5 M AHA/1 M NH_4OH solution spiked with ^{99}Mo radiotracer and calculating the concentration in each phase after reaching equilibrium with a known mass of preequilibrated resin.

First, the masses of 2-mL microcentrifuge tubes were recorded before and after the addition of approximately 0.1 g of the dry resin, and 1 mL of a 1 M NH_4OH wash was added to each. The vials were shaken by hand for 5 minutes and then centrifuged for 3 minutes at 1,500 RPM so that the liquid supernatant could be decanted, and 1 mL 1 M NH_4OH was added to the vial and allowed to sit for at least 1 hour to preequilibrate the resin. The vial was again centrifuged and the supernatant decanted. The masses of the preequilibrated vials were recorded, and the difference in mass between the dry and preequilibrated resin was used to calculate the volume of 1 M NH_4OH remaining in the vial from its density (0.9895 g/mL). Finally, 1 mL of a solution consisting of a ^{99}Mo spike in 0.5 M AHA/1 M NH_4OH with a carrier molybdenum concentration between 14 and 206 mM was added to the vials and shaken for 5 minutes at ambient temperature (25°C). Subsamples of the aqueous supernatant (300 µL) were collected after centrifuging the vials and counted on a NaI detector.

The decay-corrected count rates in the 700–900 keV window were used to calculate liquid and solid phase concentrations using Equations (5) and (6), where $[Mo]_i$ is the initial concentration of molybdenum in the aqueous phase, $[Mo]_{aq}$ is the final concentration of molybdenum in the aqueous phase, $C_{n,i}$ is the initial decay-corrected count rate in the aqueous phase, $C_{n,aq}$ is the final decay-corrected count rate in the aqueous phase, $[Mo]_r$ is the final molybdenum concentration in the resin on a volume basis, V_l is the volume of the aqueous phase, and V_r is the volume of the resin. The resin volume was calculated using the measured mass and reported resin density of 0.75 g/mL. The Langmuir isotherm (Equation [7]) was fitted to the liquid and solid phase concentrations using the least- squares method by varying the values of the fitting parameters a and b.

$$[\mathrm{Mo}]_{\mathrm{aq}} = \frac{C_{n,\mathrm{aq}}}{C_{n,i}}[\mathrm{Mo}]_i \tag{5}$$

$$[\mathrm{Mo}]_r = \frac{V_l}{V_r}([\mathrm{Mo}]_i - [\mathrm{Mo}]_{\mathrm{aq}}) \tag{6}$$

$$[\mathrm{Mo}]_r = \frac{a[\mathrm{Mo}]_{\mathrm{aq}}}{1 + b[\mathrm{Mo}]_{\mathrm{aq}}} \tag{7}$$

2.8 STEADY-STATE MULTISTAGE COUNTERCURRENT LIQUID-LIQUID EXTRACTION CALCULATIONS

In the ^{99}Mo production process being developed by Niowave, as many as 150 uranium targets will be irradiated in series each day. Following irradiation, the targets will be dissolved batchwise and the dissolver solutions will be combined and fed to the downstream continuous solvent extraction separation process. The aqueous solvent extraction product stream will then be run through an ion exchange column for final ^{99}Mo purification, with periodic elution of the retained ^{99}Mo from multiple irradiations for shipping. The ^{99}Mo concentration at each step should be as high as possible to minimize the column size required for the final purification step, and to reduce the product volume for shipping.

In order to evaluate solvent recycle as an option for increasing the concentration of ^{99}Mo in the MoLLE process streams before final purification by ion exchange, mass transport calculations were performed for an ideal steady-state multistage countercurrent solvent extraction process consisting of many centrifugal contactor banks in series. For these calculations, the aqueous feed to each bank was a fresh ^{99}Mo stream of constant composition, while the organic feed was the organic phase outlet stream from the previous bank of contactors. The distribution ratio for each equilibrium stage was assumed to be constant regardless of molybdenum concentration or phase ratio, which is valid at low molybdenum concentrations. Stream compositions and molybdenum recoveries were calculated from the molybdenum distribution ratio and the material balance for each process step.

This simplified configuration approximates the behavior of a process in which large holdup tanks containing the initial feed streams are connected to a single bank of centrifugal contactors with a total internal volume much smaller than the tanks, where the process is run repeatedly at steady state until the holdup tanks are empty. The feed tanks are then refilled, one with the organic phase from the previous run and the other with a fresh aqueous feed. Each repeat run, which corresponds to an additional contactor bank in the mass transport calculation, is referred to as a “cycle” in the discussion of these results.

3 RESULTS AND DISCUSSION

3.1 AMUSE SIMULATIONS

We simulated Niowave's uranium target feed (1.3 M UO_2^{2+}, 3 M HNO_3) in a 7 × 2 × 6 extraction, scrub (3 M HNO_3), and strip (0.01 M HNO_3) contactor bank, as shown in FIGURE 2. The flowrates have been omitted. The results demonstrate sufficient uranium extraction, minimal loss during the scrub section, and good recovery in the dilute acid strip section.

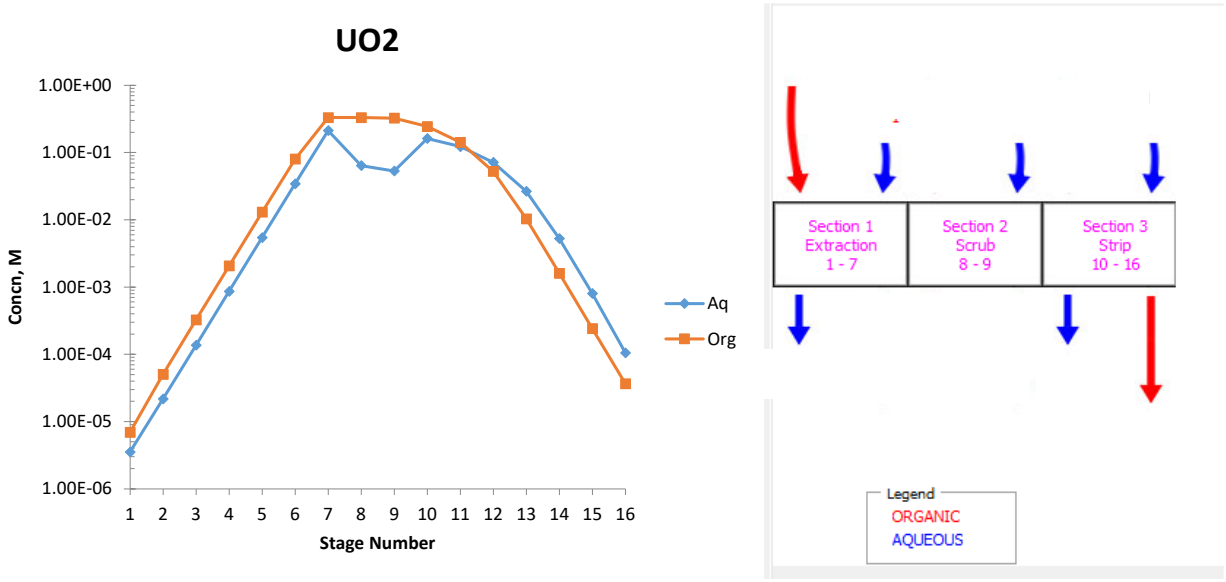

FIGURE 2 AMUSE Flowsheet for the Purification and Recovery of Uranium Using 16 Centrifugal Contactor Stages.

This flowsheet has not been optimized to decontaminate uranium from fission products, transuranics, and activation products. Additional purifications steps—such as an AHA contact to remove Pu or oxalic acid to remove Zr—may be required, depending on any decisions to manage U/Np/Pu waste streams. Technetium may require ion exchange treatment or concentrated HNO_3 contacts to remove it from the uranium product stream, depending on the concentrations and number of process cycles. A select number of contaminants such as I and Np may fractionate across this flowsheet and may exhibit different oxidation states, depending on the burnup and decay times.[10]

Preliminary experimental data obtained at Niowave showed that ^{99}Mo extracted to a relevant extent in the UREX sections (~10%). Solvent extraction literature generally reports that Mo(IV) exhibits a very weak affinity for TBP across most mild nitric acid concentrations.[11] However, co-extraction of trace ions in the presence of bulk materials from nitric acid is sometimes observed during large-scale extraction processes.[10] We simulated the extraction of Mo(VI) at trace concentrations (<0.1 mM) with and without uranium to verify whether bulk

uranium ions can co-extract Mo(IV). FIGURE 3 plots the distribution of trace Mo(VI) as a function of HNO_3. As expected, the distribution is relatively low ($D < 10^{-2}$), however, a notable increase of almost a factor of 10 is observed in the presence of 1.3 M UO_2^{2+}. TABLE 5 lists the simulated concentrations of H, Mo, and U as a function of O:A scrub ratios using 3 M HNO_3. The loaded solvent contained 0.24 M uranyl nitrate and 10^{-8} M Mo, which is typical for a two-stage batch equilibrium extraction process with an O:A of 4:1.5. The results show a decreasing trend in the distribution of Mo as the O:A is increased. Concurrently, note that approximately 5% uranium loss is expected during these scrub sections as evident by the decreasing *D* values. We conclude that high uranium concentrations can have an impact on the extraction of ^{99}Mo and that efficient nitric acid scrub sections should be considered to achieve overall recoveries of >90%.

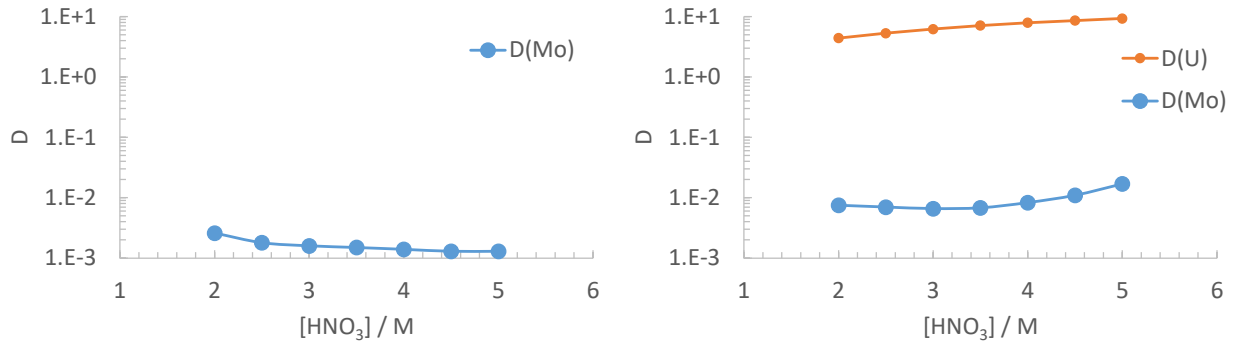

FIGURE 3 Extraction of Trace Mo(IV) into 30% TBP as a Function of Nitric Acid (left) and in the Presence of 1.3 M UO_2^{2+}(right).

TABLE 5 Distributions of H, Mo, and U from a Solvent Containing 0.24 M U and 3.2×10^{-8} M Mo, Using 3 M HNO_3.

O:A	Z	Aqueous (M)	Organic (M)
6:1	H	2.28	0.43
	Mo	2.5E-8	2.5E-10
	U	3.5E-3	6.9E-2
8:1	H	2.19	0.42
	Mo	3.3E-8	2.8E-10
	U	3.6E-3	6.9E-2
10:1	H	2.11	0.4
	Mo	4.1E-8	3.2E-10
	U	3.7E-3	6.9E-2

3.2 ANTIMONY AND TIN EXTRACTION CHEMISTRY

The extraction of Sb and Sn in processes used to separate uranium and fission products, such as the UREX process, is not as well characterized as for higher-yield elements. These fission products are relevant in the context of ^{99}Mo processing given their strong gamma emissions, relatively long half-lives (^{127}Sb $t_{½}$ = 3.8 d; ^{125}Sn $t_{½}$ = 9.6 d), and complicated aqueous speciation. In addition to obtaining experimental data on the solvent extraction of Sb and Sn by TBP, we collected literature data on both elements.[12-17] The literature data is plotted in FIGURE 4. Overall, the distribution of these elements is relatively low ($D < 10^{-2}$) and from a process standpoint these values indicate that neither Sb or Sn should extract to any reasonable extent into TBP. Scrub stages that are already implemented for U recovery would likely provide sufficient decontamination.

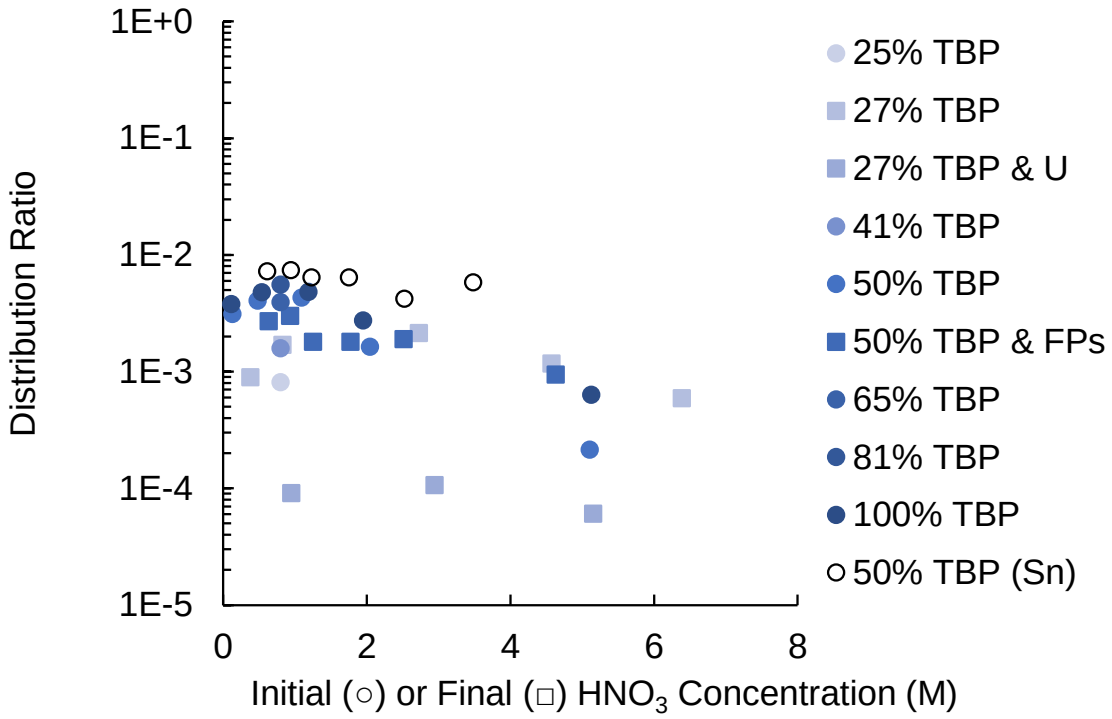

FIGURE 4 TBP Extraction Data on Sb (closed symbols) and Sn (open symbols) as a Function of Nitric Acid TBP Concentration.

The partitioning of stable Sb(V) and Sn(II) between aqueous nitric acid and either 30% TBP in dodecane or 0.4 M HDEHP in dodecane was measured by determining the final aqueous phase concentrations of each metal after reaching equilibrium. Antimony was not strongly extracted by either extractant at nitric acid concentrations of up to 4 M. The final aqueous phase Sb(V) concentrations indicate that the distribution ratios for all experimental conditions tested were less than 10^{-1}.

As shown in FIGURE 5, Sn(II) was very well extracted by HDEHP, and poorly to moderately extracted by TBP. Data for HDEHP extraction from 0.5 and 1 M HNO_3 are not shown due to problems with the quantification of tin at the very low concentrations remaining in the aqueous phase following extraction. The decrease in distribution ratio with increasing nitric acid concentration for TBP suggests that Sn(II) has a low tendency to form neutral adducts, which is consistent with most low-valence ion extraction behavior. The extraction of Sn(II) by HDEHP observed here is much greater than that reported previously[18], perhaps due to challenges in maintaining the lower tin oxidation state in a strongly oxidizing nitric acid environment. The Sn(II) spike solution prepared as described in the methods section was unstable and formed a precipitate after resting for less than 24 hours. This precipitate likely consists of insoluble Sn(IV) hydrolysis products. The distribution of tin between its dominant solution phase oxidation states, II and IV, was not controlled in this work. Prior data for the extraction of Sn(II) by TBP could not be located in the open literature, likely due to its poor stability in nitric acid solution.

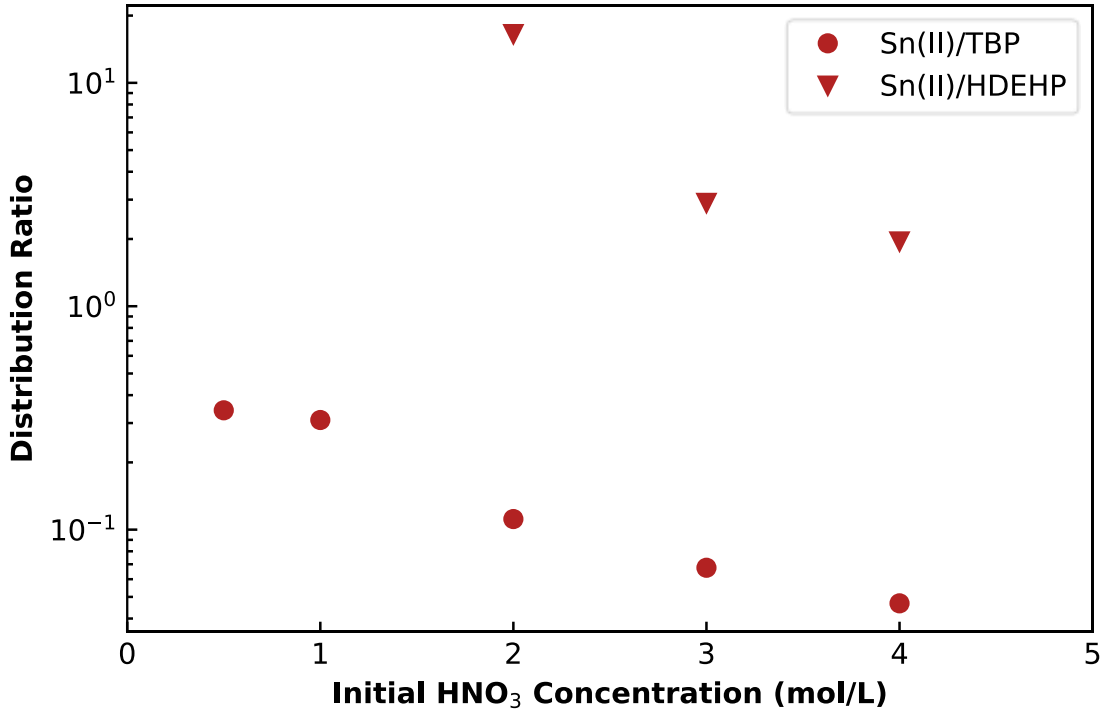

FIGURE 5 Sn(II) Distribution Ratios for 30 v/v% TBP and 0.4 M HDEHP in Dodecane at Various Initial Aqueous HNO_3 Concentrations.

3.3 HDEHP FISSION PRODUCT EXTRACTION AND STRIPPING

The ^{99}Mo separation and purification process proposed for use by Niowave, Inc., relies on extracting molybdenum and selected fission product impurities by HDEHP from nitric acid, followed by selectively stripping molybdenum by AHA. The aqueous feed to the HDEHP extraction section consists of the raffinate from a preceding UREX section. The extraction of

fission products by TBP from molar nitric acid, as used in the UREX process, is one of the most well-characterized separations in nuclear science. The extraction of fission products by HDEHP, while also important, has not been as extensively characterized for nitric acid concentrations between 1 and 5 M. Data have not been reported in the literature for the 0.4 M HDEHP/dodecane system used here. Furthermore, distribution data for the stripping of fission products by AHA from an HDEHP organic phase are not available.

FIGURE 6 shows measured distribution ratios for the extraction of six fission products by 0.4 M HDEHP in dodecane up to 4 M HNO_3. These radionuclides were the only components with observable gamma peaks in both the equilibrium organic and aqueous phases. ^{103}Ru and ^{140}Ba, which were detectable in the initial solution, were both so poorly extracted that they were undetectable in the final organic phase. The distribution ratios for these elements are estimated from the organic phase MDA to be less than 10^{-2}. The high-oxidation-state elements—Mo(VI), Nb(V), and Zr(IV)—are nearly quantitatively extracted at all nitric acid concentrations. Iodine, which primarily exists as molecular I_2 under acidic conditions, does not demonstrate a preference for either the aqueous or the organic phases. This behavior is consistent with that expected for a small, nonpolar compound that is neither strongly hydrated nor extracted. Finally, the trivalent lanthanides were poorly extracted except at very low nitric acid concentrations, which is consistent with the cation-exchange mechanisms of HDEHP. The greater extraction of the marginally smaller cerium cation over lanthanum reflects the general selectivity of HDEHP for high-charge-density cations. Overall, the extraction trends in FIGURE 6 demonstrate that there is no benefit to increasing the acid concentration in the UREX raffinate, which is at approximately 1 M HNO_3 based on AMUSE simulations, prior to contacting it with HDEHP.

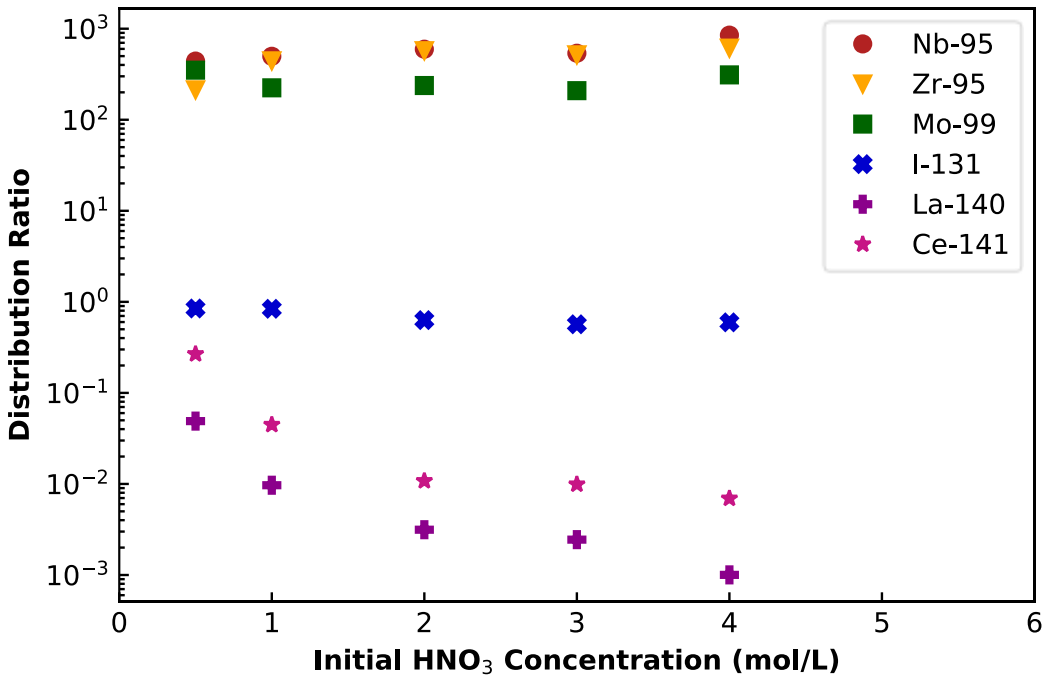

FIGURE 6 Fission Product Distribution Ratios under Extraction Conditions for the 0.4 M HDEHP in Dodecane System.

The distribution ratios of fission products under MoLLE stripping conditions are shown in FIGURE 7. Due to decay of the initial spike, the only detectable fission products in these experiments were ^{95}Nb, ^{95}Zr, ^{103}Ru, and ^{141}Ce. Unlike in the experiments that measured fission product distribution ratios under extraction conditions, all of these radionuclides were detected in both phases under stripping conditions. The addition of AHA to the aqueous phase shifts the affinity of molybdenum and niobium from the organic phase to the aqueous phase through the formation of stable aqueous metal-AHA complexes.[4] These data show that the AHA strip improves the extraction of ruthenium and cerium by HDEHP compared with their behavior under extraction conditions due to the absence of competing HNO_3. However, their distribution ratios are not as high as would be expected at pH 4, the approximate pH of the AHA phase, which suggests the formation of additional aqueous complexes in this system. The extraction of zirconium is substantially the same under both extraction and stripping conditions. The optimum AHA concentration for stripping appears to be 0.5 M, near the knee of the molybdenum distribution ratio curve.

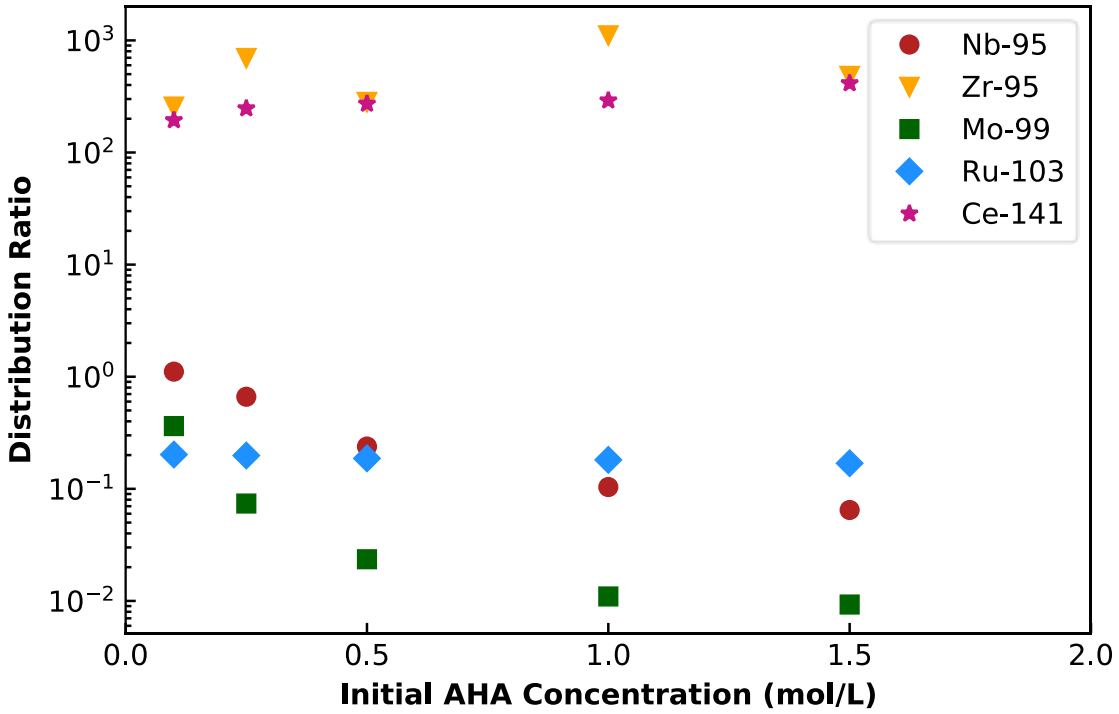

FIGURE 7 Fission Product Distribution Ratios under Stripping Conditions for the 0.4 M HDEHP in Dodecane System.

One potential barrier to the use of AHA to selectively strip molybdenum from an HDEHP organic phase lies in the formation of persistent emulsions after vigorously mixing the organic and aqueous phases. This phenomenon was observed while performing ^{99}Mo distribution ratio measurements under stripping conditions, where a white emulsion formed at the interface between the transparent aqueous and organic phases. This emulsion, which did not contain any

^{99}Mo, did not coalesce after either 1 hour or 10 minutes of centrifugation at 2,000 RPM. This undesirable behavior was further explored in metal-free systems, as described in Section 3.6.

3.4 NIOBIUM AND CONCENTRATION COLUMN DEVELOPMENT

Results obtained at Niowave while processing irradiated targets demonstrated that Nb has a tendency to follow Mo through UREX and MoLLE. Niobium is also adequately retained by an anion exchange resin under alkaline conditions where MoO_4^{2-} is formed. Thus, niobium presented a significant technical challenge that required a more specific decontamination approach. We explored a number of precipitation steps that employed either $Fe(OH)_3$ or $Gd(OH)_3$ to carry Nb in alkali conditions.[19] However, we found that ^{99}Mo co-precipitated with $Gd(OH)_3$ to a small extent and that iron exhibited some solubility in alkali conditions (pH > 13).[20] We pursued the removal of Nb using the concentration column. Anion-exchange resins exhibit a high affinity for Mo in 3–8 M HCl due to the multiple anionic chloride complexes of molybdenyl, whereas Nb exhibits a minimum in partitioning between 4 and 8 M HCl.[21, 22] The separation bands of Nb and Mo can be resolved even further by adding oxalic acid or hydrogen peroxide.[23] Leveraging this chemistry, we targeted the complete removal of Nb using HCl and oxalic acid.

Using the irradiated Mo disc stock solution (comprised of ^{99}Mo, ^{95}Nb, and ^{95}Zr) that was acidified with HNO_3 and processed by MoLLE, the AHA strip solution was contacted with NH_4OH and fed through 1 g of pre-equilibrated AG-MP1 resin. The results are shown in FIGURE 8. The HCl/oxalic acid wash step had a significant impact on Nb without eluting the retained Mo. Over 30 mL of solution was required for complete removal. A 4 M HCl wash was included to remove residual oxalic acid. Finally, the 1 M/1 M NaOH/NaCl step recovered the Mo in approximately 10 mL. The results indicate that Nb/Mo separation can be achieved on an anion exchange column using HCl and oxalic acid. However, it was critical that this elution profile be tested in the presence of other fission products in addition to Nb and Mo.

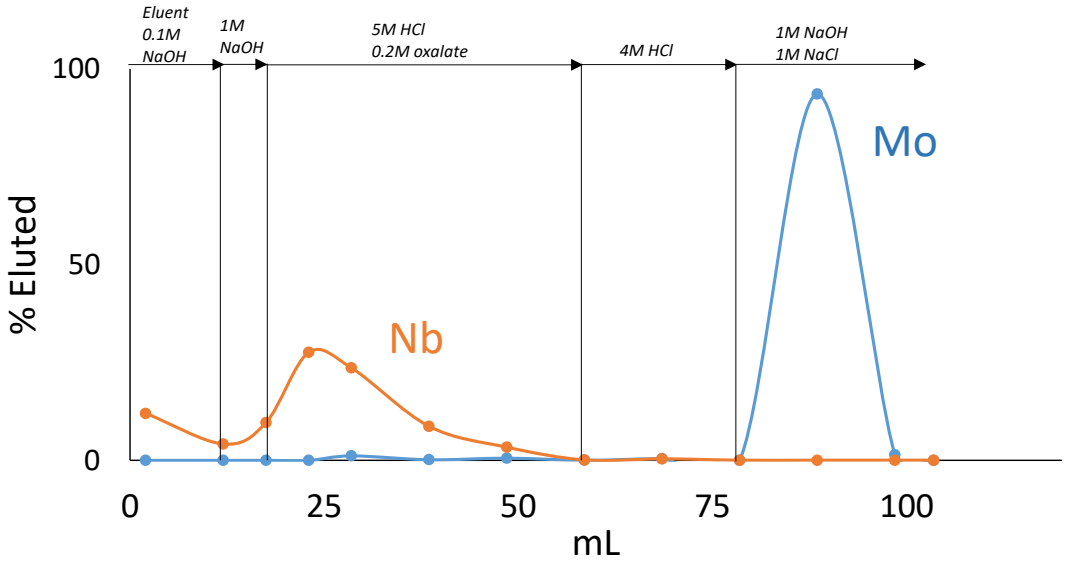

FIGURE 8 Elution Profile for Nb and Mo across an Anion Exchange Column.

3.5 PROCESS DEMONSTRATION USING LEU

In order to evaluate and refine the process chemistry under realistic experimental conditions, a surrogate dissolved target solution containing 1.3 M uranyl nitrate and representative fission products was prepared and the purification process was performed on the surrogate twice at bench scale.

The focus of the first experiment was on the chemistry of the anion exchange column and ensuring that the ^{99}Mo product was fully decontaminated from minor impurities. The elution profile generated from this experiment is shown in Figure 9. Traces of Np, Te, Zr, and Ce were removed after the initial eluant load and with increasing concentrations of NH_4OH up to 1 M. The HCl/oxalic acid wash steps eluted Nb in approximately 40 Ml, which is consistent with the results presented in FIGURE 8. The 4 M HCl wash step unexpectedly targeted residual ^{131}I. The ^{99}Mo recovery step using 1 M NaOH/1 M NaCl was complete after one wash. The HPGe spectra of the UREX feed, raffinate, and ^{99}Mo product are plotted in Figure 10.

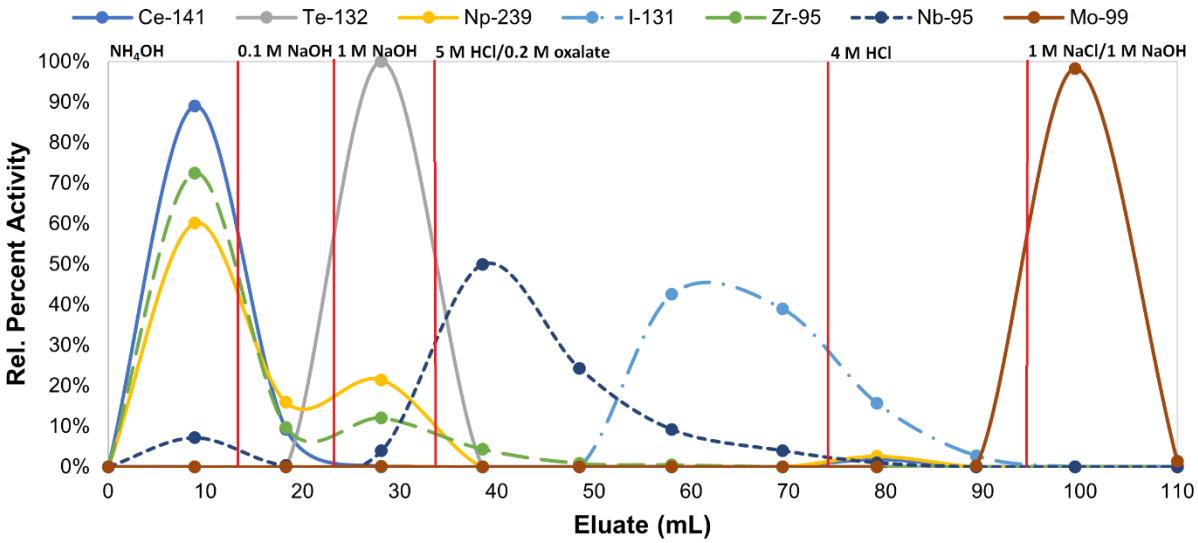

Figure 9 Elution Profile of Selected Fission Products across an Anion Exchange Column.

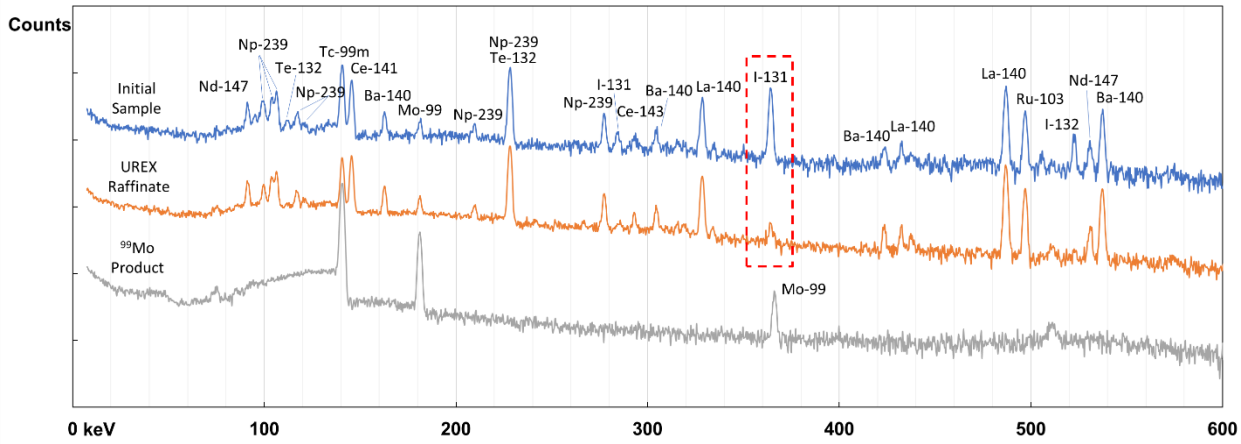

Figure 10 HPGe Spectra of the Initial Feed Solution, the UREX Raffinate, and the ^{99}Mo Product Derived from the Concentration Column.

Thiocyanate extraction, a standard method for determining if ^{99}Mo meets radionuclidic purity specifications, was performed on the resulting ^{99}Mo product. The ratio of the ^{103}Ru MDA to the ^{99}Mo activity decay corrected to 3 days after the end of bombardment was determined to be 3×10^{-4}. The product specification for commercially available ^{99}Mo is $<5 \times 10^{-5}$. It is possible that the ^{103}Ru activity in the ^{99}Mo product falls below this limit; however, the low specific activity of the initial sample means that it cannot be distinguished from background. The total ^{99}Mo concentration was less than the threshold quantity of 100 mCi/mL described in the quality control procedure analysis.

The process was performed a second time to gain a more detailed understanding of where each fission product was going in the course of the experiment. A detailed breakdown of the compositions of each process stream and the column elution profile is reported in Figures 11–13 and Table 6 as percentages of the decay corrected activities of each radionuclide in the initial surrogate solution. These percentages do not always add up to 100% due to large variations in the background activities of each sample. However, they are generally within 10% of the initial activities—except for ^{239}Np, which is low following the HDEHP extraction step, likely due to the very high background activity in the exiting aqueous stream.

The results of this second experiment suggest that the overall process is very effective, resulting in >95% recovery of the ^{99}Mo. No fission product impurities were detected in the gamma spectrum of the ^{99}Mo product, although this does not necessarily mean that the ^{99}Mo meets standard radiochemical and radionuclidic purity specifications for commercially available ^{99}Mo. Most of the decontamination of the ^{99}Mo from the highest activity impurities took place during the initial HDEHP extraction. The impurities remaining following the AHA strip were at low activities relative to their initial amounts, and consisted primarily of ^{95}Nb with detectable gamma peaks for ^{132}Te, ^{239}Np, and ^{95}Zr. ^{141}Ce and ^{131}I were not observed in any of the column washes in this second run.

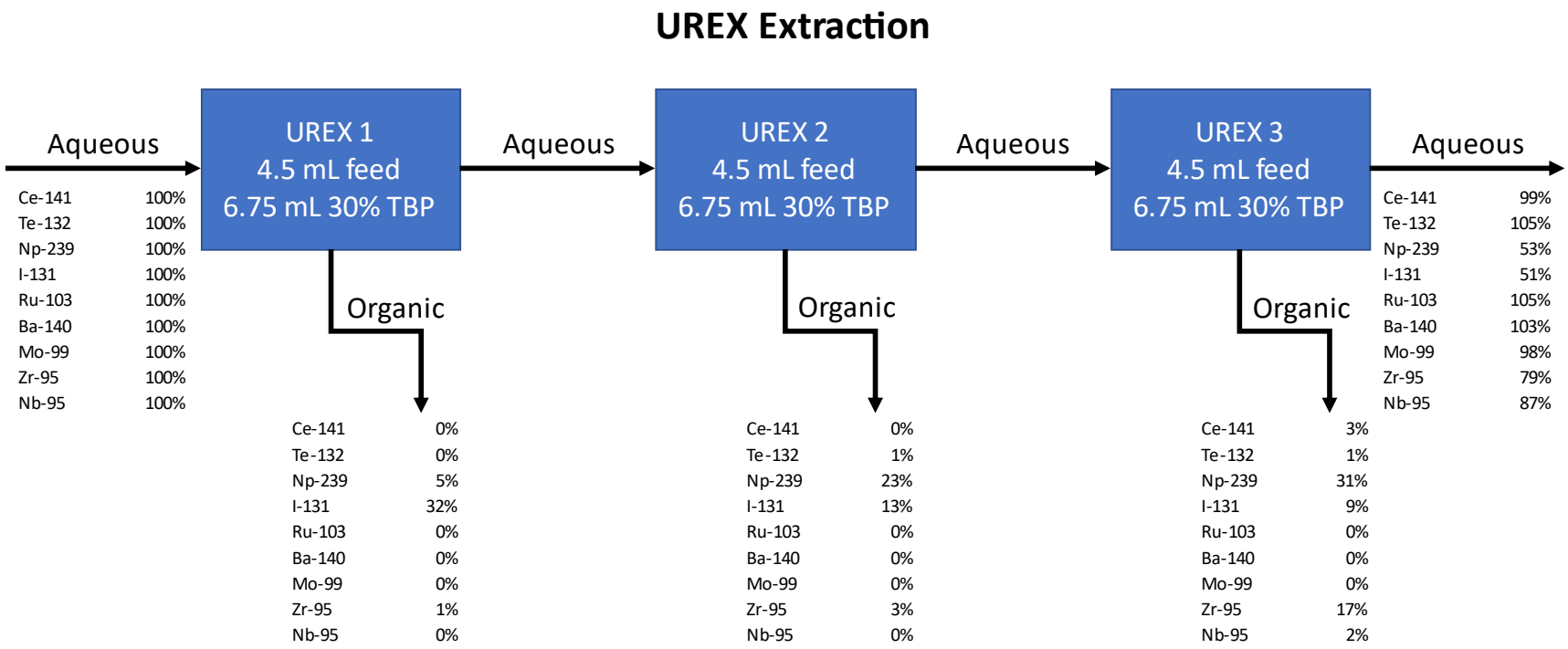

FIGURE 11 Fission Product Fractionation across the UREX Circuit.

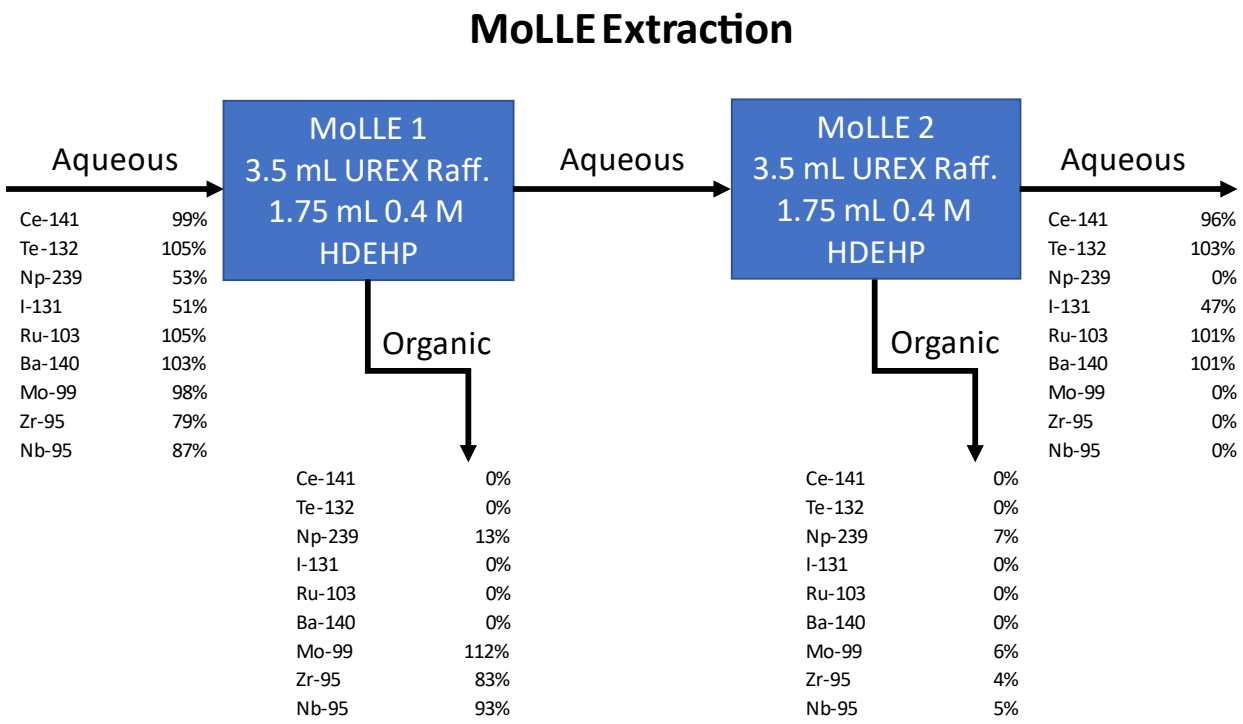

FIGURE 12 HDEHP Contacts with a UREX Raffinate.

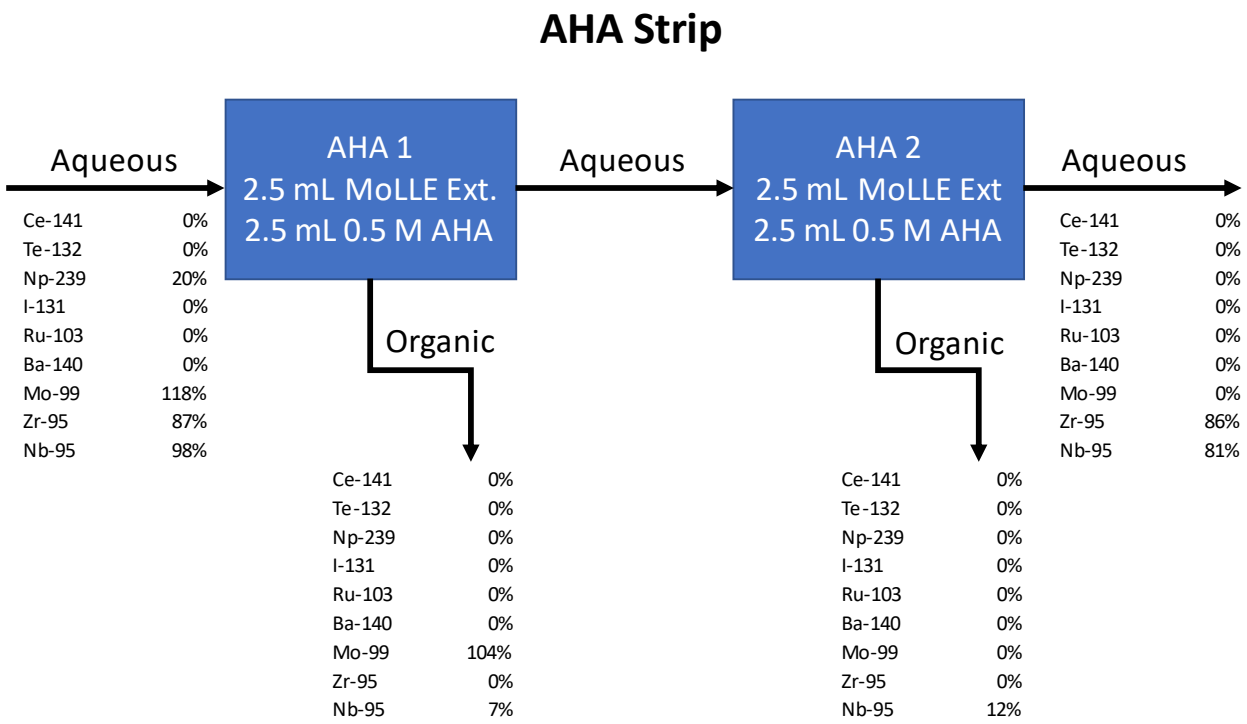

FIGURE 13 AHA Contacts with a Loaded HDEHP Solvent (Figure 12).

TABLE 6 Percent Activity Fractionation across the Concentration Column.

Volumes and Tracers	NH_4OH	NaOH	HCl/Ox	HCl/Ox	HCl/Ox	HCl/Ox	HCl	HCl	NaCl/NaOH	NaCl/NaOH
Amount Added (mL)	5	10	10	10	10	10	10	10	10	10
Total Volume (mL)	5	15	25	35	45	55	65	75	85	95
^{141}Ce	ND[a]	ND	ND	ND	ND	ND	ND	ND	ND	ND
^{132}Te	0.2%	ND	ND	ND	ND	ND	ND	ND	ND	ND
^{239}Np	0.9%	2%	ND	ND	ND	ND	ND	ND	ND	ND
^{131}I	ND	ND	ND	ND	ND	ND	ND	ND	ND	ND
^{103}Ru	ND	ND	ND	ND	ND	ND	ND	ND	ND	ND
^{140}Ba	ND	ND	ND	ND	ND	ND	ND	ND	ND	ND
^{99}Mo	ND	ND	ND	ND	ND	ND	ND	ND	98%	1%
^{95}Zr	0.1%	0.1%	ND	ND	ND	ND	ND	ND	ND	ND
^{95}Nb	0.4%	7%	6%	2%	1%	0.7%	0.2%	ND	ND	ND

[a] ND = not detected at a level greater than 0.05% of the initial decay corrected activity.

Iodine, neptunium, and zirconium were the primary fission product impurities extracted by TBP during the UREX section of the ^{99}Mo purification process (Figure 11). ^{99}Mo decontamination from cerium, tellurium, ruthenium, and barium by HDEHP extraction was excellent, leaving only zirconium, niobium, and neptunium at significant activities in the organic phase with the ^{99}Mo (Figure 12). ^{99}Mo was decontaminated from most of the remaining zirconium and niobium by AHA stripping (Figure 13).

3.6 PHASE DISENGAGEMENT IN HDEHP-AHA SYSTEMS

Although the stripping of ^{99}Mo from an HDEHP organic phase by 0.5 M AHA is a chemically favorable process, complete separation of the two phases after mixing was observed to be inconsistently slow in both batch distribution studies and bench-scale process tests. To further understand and characterize the phase disengagement behavior of an HDEHP-containing organic phase and an AHA-containing aqueous phase, test tube phase disengagement experiments were performed under a variety of experimental conditions to determine the effect of different variables on the value of the dimensionless dispersion number. Examples of organic continuous and aqueous continuous dispersions following bulk phase separation are shown in Figure 14. Both phases in organic continuous dispersions (left) appeared transparent following bulk phase separation, although aqueous bubbles in the organic phase were observed during separation. The aqueous phase remained cloudy in aqueous continuous dispersions (right) following bulk phase separation. The results of these phase disengagement tests are given in TABLE . Experimental parameters varied were $NaNO_3$ or HNO_3 concentration in the aqueous phase, AHA concentration in the aqueous phase, age of the AHA solution (prepared that day or aged 24 hours), and HDEHP pre-equilibration conditions (no pre-equilibration, pre-equilibration with 1 or 4 M HNO_3). The dispersion number for the first shake is N_{D1}, while the dispersion number for the second shake is N_{D2}.

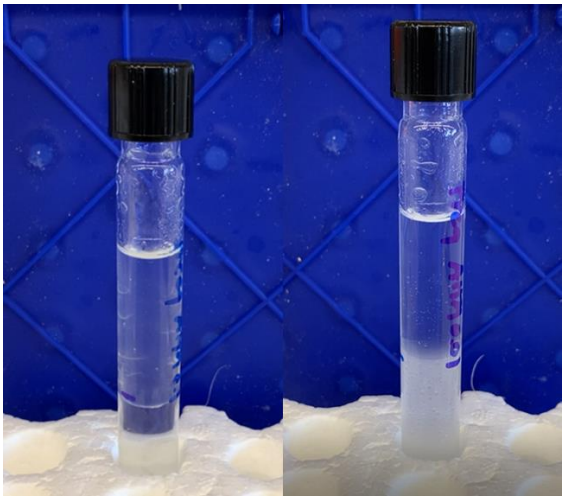

FIGURE 14 Photograph of Two-phase Disengagement System: Organic Continuous Dispersions (left) and Aqueous Phase (right).

TABLE 7 Phase Disengagement Tests Showing the Value of the Dimensionless Dispersion Number.[a]

	Aqueous Phase				
ID	[AHA]	[$NaNO_3$]	[HNO_3]	N_{D1}	N_{D2}
Fresh AHA					
A	0.5	0	0	2.3E-03	3.2E-04
B	0.5	0	0	3.1E-03	3.8E-04
C	0.5	0	0.1	2.2E-03	2.3E-03
D	0.5	0	0.01	2.6E-03	1.9E-04
E	0.25	0	0	3.3E-03	1.0E-04
F	0.25	0	0.1	2.1E-03	2.1E-03
Aged AHA					
G	0.5	0	0	9.6E-04	4.1E-04
H	0.5	0	0	3.1E-03	5.0E-04
Fresh AHA					
I	0.5	0	0	3.8E-03	1.2E-04
J	0.5	0	0	4.0E-04	2.4E-04
K	0.5	0.05	0	7.9E-04	2.7E-03
L	0.5	0.1	0	2.6E-03	1.0E-03
M	0.5	0.5	0	2.5E-03	2.0E-03
N	0.5	1	0	1.9E-03	1.7E-03

[a] Phase disengagement tests showed that the value of the dimensionless dispersion number was optimal at elevated ionic strength, at least 0.1 M HNO_3 or 0.5 M $NaNO_3$. A dimensionless dispersion number in green indicates excellent separation, yellow is good or fair separation, and red is poor separation based on the metrics outlined in [8]. Dark blue indicates no pre-equilibration, medium blue indicates pre-equilibration with 1 M HNO_3, and light blue indicates pre-equilibration with 4 M HNO_3.

All organic continuous dispersions (dispersions consisting of aqueous droplets in a continuous organic phase) were observed to separate phases rapidly and were usually formed following the first shake of a sample. In contrast, aqueous continuous dispersions were very slow to separate and usually formed during the second shake. The only exceptions were Sample K, where an organic continuous dispersion formed during the second shake, and Samples C, F, M, and N, which appeared to form only organic continuous dispersions. This behavior demonstrates the sensitivity of this experiment to small changes in shaking technique and time. The HDEHP pre-equilibration conditions and AHA concentrations appeared to have a minimal impact on phase disengagement, while aging of the AHA solution seemed to improve phase disengagement in aqueous continuous dispersions.

The formation of unfavorable aqueous dispersions is prevented by the addition of ionic species to the aqueous phase. Samples with at least 0.1 M HNO_3 or 0.5 M $NaNO_3$ separated rapidly even after vigorous shaking (at least 5 minutes of shaking by hand) and aging of the sample. Distribution ratios for selected fission products were unaffected by the addition of 0.1 M HNO_3 to the AHA strip, even when the AHA solution was aged for 8 days, as shown in FIGURE . The distribution ratios for selected fission products in 0.4 M HDEHP were substantially the same for a freshly prepared 0.5 M AHA aqueous phase with and without HNO_3, as well as a 0.5 M AHA aqueous phase with HNO_3 that had been aged for 8 days. AHA is known to undergo acidic hydrolysis in the presence of HNO_3.[24] However, the measured distribution ratios show that this hydrolysis occurs slowly enough in 0.1 M HNO_3 that the ^{99}Mo recovery during the AHA strip is unaffected. The addition of HNO_3 to the AHA strip as needed to improve the phase disengagement characteristics of the system is not expected to have adverse effect on the separations chemistry.

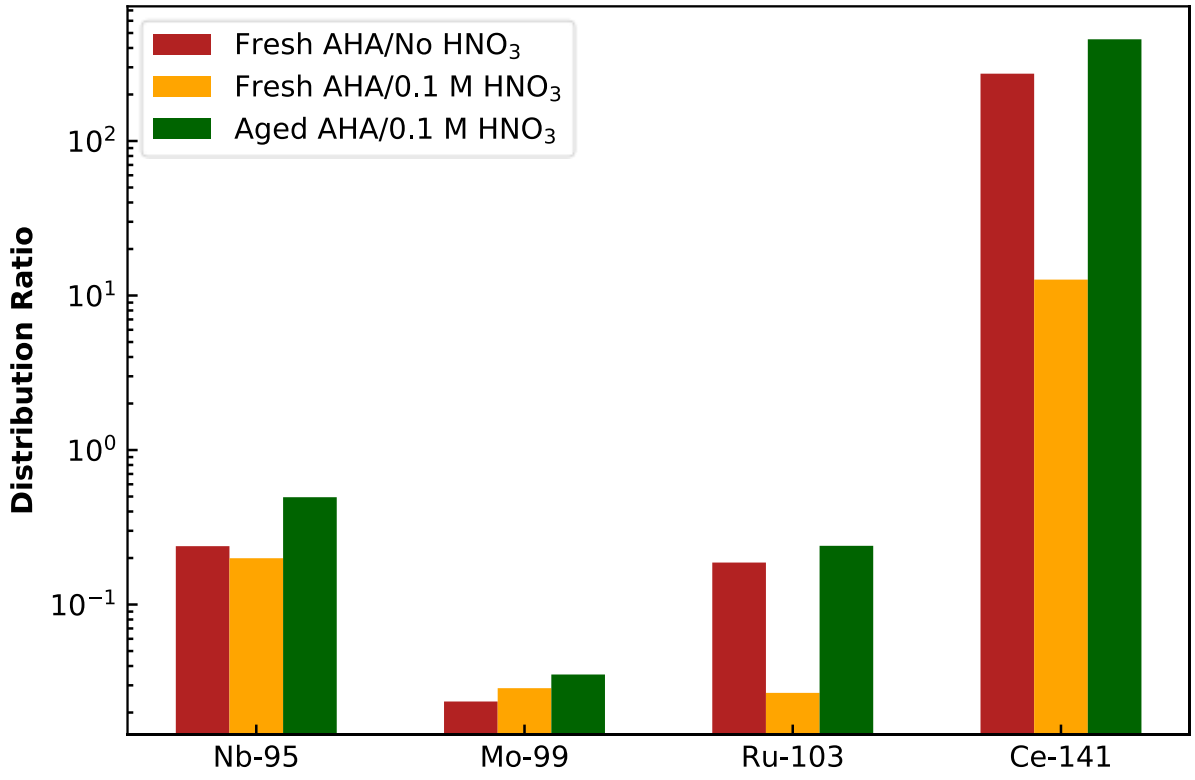

FIGURE 15 Distribution Ratios for Selected Fission Products in 0.4 M HDEHP.

3.7 ^{99}MO SOLID PHASE ADSORPTION BY AN ANION EXCHANGE POLYMER RESIN

The Langmuir isotherm for molybdenum adsorption by AG 1-X8 resin (hydroxide form; 200–400 mesh) from 0.5 M AHA/1 M NH_4OH solution at 25°C is shown in FIGURE . The values for *a* and *b* determined by least-square fitting are *a* = 684 L aqueous phase/L resin and *b* = 0.859 L aqueous phase/mmol Mo. This corresponds to a solid phase monolayer concentration of 769 mmol Mo/L resin at saturation.

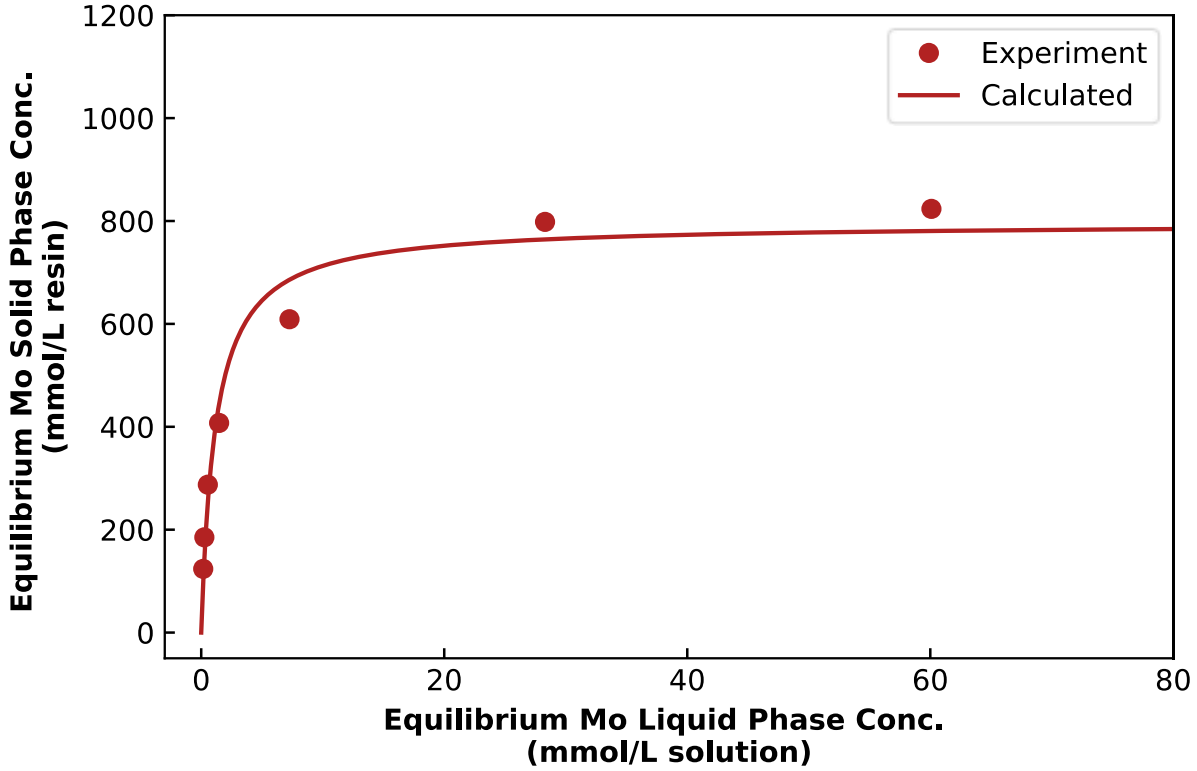

FIGURE 16 Langmuir Adsorption Isotherm for Mo Uptake by AG 1-X8 from 0.5 M AHA/1 M NH_4OH Fitted to Equilibrium Adsorption Data Collected at 25°C.

Figure 14 compares the uptake of molybdenum from NH_4OH solution with uptake from 0.1 M NaOH by plotting the Langmuir isotherm for both. Langmuir isotherm parameters for the 0.1 M NaOH system had been measured previously for the same anion exchange resin.[25] The adsorption curve in Figure 17 shows that molybdenum uptake by AG 1-X8 is substantially higher from 0.1 M NaOH compared with the NH_4OH solution tested in this work. These results suggest that loading the ^{99}Mo on the anion exchange column in 0.1 M NaOH would be preferable to the current practice of loading in 0.01 M NH_4OH.

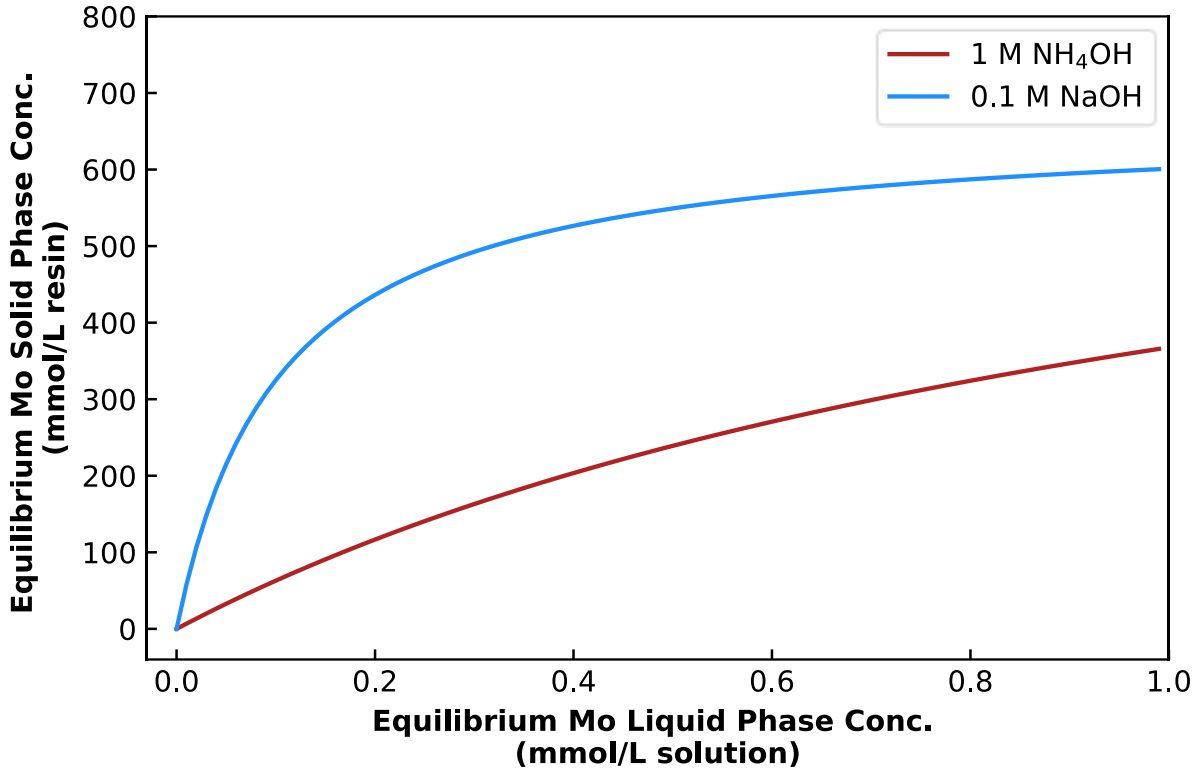

FIGURE 17 Molybdenum Uptake by AG 1-X8 from 0.1 M NaOH Compared with 1 M NH_4OH.

3.8 SOLVENT RECYCLE CALCULATIONS FOR INCREASING MOLYBDENUM CONCENTRATION

Mass transport calculations for an ideal, steady-state molybdenum solvent extraction process consisting of multistage countercurrent centrifugal contactor banks in series show considerable losses of material as the number of cycles (banks) increases. These results are shown in FIGURE . Increasing the number of stages in each cycle from 2 to 5 does not improve the overall molybdenum recovery due to the elevated amount of molybdenum entering each cycle beyond the first in the organic feed. Losses expected for 100 cycles, corresponding to the more than 100 target batches expected to be processed by Niowave each day, exceed 20% even under these ideal conditions. Accounting for the reduced mass transport efficiencies observed in real liquid–liquid extraction equipment, this number would be expected to be increased significantly in a real process. These calculations demonstrate that increasing the ^{99}Mo concentration in the final product should be achieved instead by decreasing the organic to aqueous (O:A) phase ratio or using a concentration column.

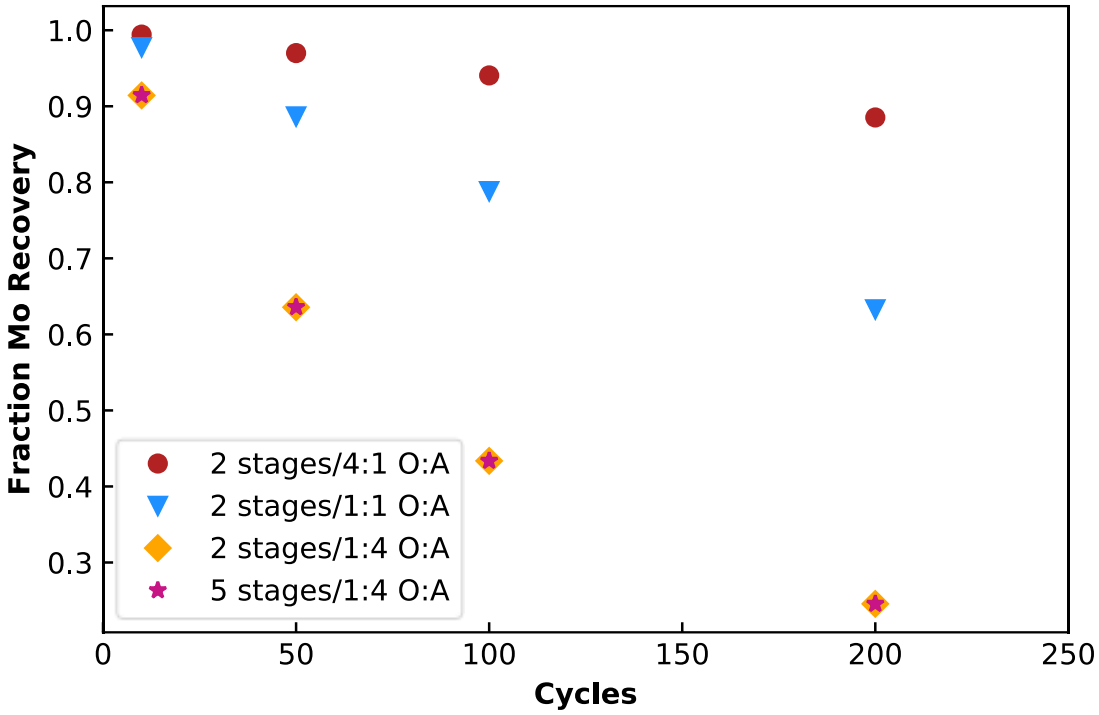

FIGURE 18 Fractionation of Mo after a Series of Cycles during Solvent Concentration in HDEHP from Nitric Acid.

4 CONCLUSION

This report summarizes an extensive experimental campaign with supporting chemical simulation software to develop and optimize solvent extraction/ion exchange process chemistry for the recovery of μCi-quantities ^{99}Mo from LEU targets. The process comprises UREX for the removal of bulk uranium, MoLLE for the recovery of ^{99}Mo, and a concentration column to concentrate and further purify ^{99}Mo from trace fission products and actinides. Each process leg was evaluated with respect to flowrates, stages, concentrations, column material, and eluents to deliver pure ^{99}Mo derived from an irradiated uranium solution. UREX was simulated in AMUSE using counter-current centrifugal contactors and results show that efficient scrub sections are important to minimize losses of ^{99}Mo. Antimony and tin, which are not well characterized within UREX, were experimentally investigated under the process conditions and show a weak affinity for TBP but potentially could extract into HDEHP. More work is needed to resolve the extraction behavior using tracers.

The novel MoLLE process was investigated with respect to fission product extraction, optimization, and solvent characterization. The results show that ^{99}Mo is efficiently extracted into HDEHP from dilute HNO_3 along with a select number of ions including Nb, Zr, I, Te, and Np. The AHA strip section primarily targets Mo and Nb where the ideal AHA concentration is >0.5 M. Increasing the acidity of the strip solution to pH 1 improved phase disengagement. For a final purification and concentration step, Mo can be purified on an anion exchange platform after the formation of MoO_4^{2-} using NaOH. Hydroxide washes removed residual Zr, Te, and Np. Hydrochloric acid in combination with oxalic acid removed Nb and traces of I; Mo can be recovered in 1 M/1 M NaOH/NaCl. The process was demonstrated twice using irradiated LEU targets and resulted in good recoveries (>90%) of high-specific-activity, high-purity ^{99}Mo. The process development and optimization is warranted in order to resolve the effects, if any, of multiple batches of ^{99}Mo across the concentration column. Larger concentrations of fission products (equivalent to Ci of ^{99}Mo) may require additional purification steps.

5 REFERENCES

1. Starovoitova, V.N., L. Tchelidze, and D.P. Wells, *Production of medical radioisotopes with linear accelerators.* Applied Radiation and Isotopes, 2014. **85**: p. 39-44.
2. Youker, A.J., et al., *Fission-Produced Mo-99 Without a Nuclear Reactor.* Journal of Nuclear Medicine, 2017. **58**(3): p. 514-517.
3. Wu, D., S. Landsberger, and G.F. Vandegrift, *Progress in chemical treatment of LEU targets by the modified CINTICHEM process*, in *19th International Meeting on Reduced Enrichment for Research and Test Reactors*. 1996: Seoul, South Korea.
4. Breshears, A.T., et al., *Synthesis of hexavalent molybdenum formo- and aceto-hydroxamates and deferoxamine via liquid-liquid metal partitioning.* Inorganica Chimica Acta, 2018. **473**: p. 102-111.
5. Gelis, A.V. and M.A. Brown, *Molybdenum recovery from aqueous nitric acid solution by solvent extraction*. 2019: US.
6. Gelis, A.V., et al., *Closing the Nuclear Fuel Cycle with a Simplified Minor Actinide Lanthanide Separation Process (ALSEP) and Additive Manufacturing.* Scientific Reports, 2019. **9**(1): p. 12842.
7. Tkac, P., et al., *Side-reaction products identified for photo-nuclear production of99Mo.* Journal of Radioanalytical and Nuclear Chemistry, 2020.
8. Leonard, R.A., *Solvent Characterization Using the Dispersion Number.* Separation Science and Technology, 1995. **30**(7-9): p. 1103-1122.
9. Gilmore, G.R., *Statistics of Counting*, in *Practical Gamma-Ray Spectrometry*. 2008. p. 101-129.
10. Vandegrift, G., F., et al., *Designing and Demonstration of the UREX+ Process Using Spent Nuclear Fuel*, in *ATALANTE 2004*. 2004: Nimes, France.
11. Braun, T. and G. Ghersini, *Extraction Chromatography*. Vol. 2. 1975, New York, N.Y.: American Elsevier Publishing Company.
12. Svantesson, I., et al., *Distribution Ratios and Empirical Equations for the Extraction of Elements in PUREX High Level Waste Solution: I: TBP.* Journal of Inorganic and Nuclear Chemistry, 1979. **41**: p. 6.
13. Svantesson, I., et al., *Distribution Ratios and Empirical Equations for the Extraction of Elements in PUREX High Level Waste Solution II: HDEHP.* Journal of Inorganic and Nuclear Chemistry, 1980. **42**: p. 6.
14. Alian, A. and A. Haggag, *Extraction and Separation of antimony(III) and (V) by a Liquid Cation-Exchanger HDEHP*. Journal of Radioanalytical Chemistry, 1974. **20**: p. 13.
15. Fujii, T., et al., *Extraction Study for TRUEX Process Using Short-Lived Radionuclides Prodced by Neutron Irradiation of Uranium.* Solvent Extraction and Ion Exchange, 2002. **20**: p. 26.
16. Kimura, K., *Extraction Studies on the System between Bis (2-ethyl hexyl)-Orthophosphoric Acid and Hydrochloric Acid (I).* Bulletin of the Chemical Society of Japan, 1960. **33**: p. 8.
17. Lakaev, V.S. and V.S. Smelov, *Extraction of Antimony from Nitric Acid Solutions Using Tributyl Phosphate II* Soviet Radiochemistry (English Translation), 1989. **30**: p. 3.
18. LaFleur, P.D. and D.A. Becker, *Activation Analysis Section: Summaries of Activities*. 1970, U.S. Department of Commerce: National Bureau of Standards.
19. Sabel'nikov, A.V., et al., *Preparation of 99Mo and 99m Tc by 100Mo(γ,n) photonuclear reaction on an electron accelerator, MT-25 microtron.* Radiochemistry, 2006. **48**(2): p. 191-194.
20. Liu, X. and F.J. Millero, *The solubility of iron hydroxide in sodium chloride solutions.* Geochimica et Cosmochimica Acta, 1999. **63**(19/20): p. 3487-3497.
21. Kraus, K.A., F. Nelson, and G.E. Moore, *Anion-exchange Studies. XVII Molybdenum(VI), Tungsten(VI), and Uranium(VI) in HCl and HCl-HF Solutions.* Analytical Chemistry, 1955. **77**: p. 3972 - 3977.
22. Wish, L., *Anion Exchange Behavior in Mixed Acid Solutions and Development of a Sequential Separation Scheme.* Analytical Chemistry, 1959. **31**(3): p. 326 - 330.
23. Bandi, W.R., et al., *Anion Exchange Separation of Zirconium, Titanium, Niobium, Tantalum, Tungsten, and Molybdenum.* Analytical Chemistry, 1961. **33**(9): p. 1275 - 1278.
24. Chung, D.Y. and E.H. Lee, *Kinetics of the Hydrolysis of Acetohydroxamic Acid in a Nitric Acid Solution.* Journal of Industrial Engineering Chemistry, 2006. **12**(6): p. 5.
25. Stepinski, D.C., et al., *Optimization of SHINE Process: Design and Verification of Plant-Scale AG 1 Anion-Exchange Concentration Column and Titania Sorbent Pretreatment*. 2016, Argonne National Laboratory.

Chemical & Fuel Cycle Technologies Division
Argonne National Laboratory
9700 South Cass Avenue, Bldg. 205
Lemont, IL 60439-4832

www.anl.gov